



Homogeneous diffusion layer model of dissolution incorporating the initial transient phase

Jakub Cupera^{a,b,*}, Petr Lansky^{a,b}

^a Department of Mathematics and Statistics, Faculty of Science, Masaryk University, Kotlarska 2, 611 37 Brno, Czech Republic

^b Institute of Physiology, Academy of Sciences of the Czech Republic, Videnska 1083, 142 20 Prague 4, Czech Republic

ARTICLE INFO

Article history:

Received 2 February 2011

Received in revised form 24 May 2011

Accepted 24 May 2011

Available online 14 June 2011

Keywords:

Dissolution

Sigmoidal profile

Random lag time

Dissolution variability

ABSTRACT

Purpose of this paper is to describe characteristic features of dissolution data by using homogeneous model of dissolution with initial transient phase. To achieve the goal we consider a random lag time before the homogeneous phase of the dissolution begins. The resulting dissolution profiles are characterized by sigmoidal shape commonly observed in empirical dissolution data. Furthermore, probability distribution of repeated measurements at fixed time is deduced from the model and function describing variability of the data in dependency on time is proposed. Three examples with normal, exponential and gamma probability distribution of the lag time are presented. All the models are pairwise compared with the Weibull function with high similarity between them. The result offers an alternative interpretation for the frequently found fit of the Weibull model to experimental data.

© 2011 Elsevier B.V. All rights reserved.

1. Introduction

Disadvantage of all the classical models of dissolution is assumption of identical initial conditions for each experiment, to be more specific, the initial time instant is always set to zero (see e.g. Costa and Lobo, 2001; Dokoumetzidis and Macheras, 2006; Macheras and Iliadis, 2006; Polli et al., 1997). However, it usually requires some time until a thin diffusion layer is formed around the solid surface of the drug and through which the molecules of the solvent diffuse to the bulk aqueous phase (see e.g. Dokoumetzidis and Macheras, 2006; Noyes and Whitney, 1897; Macheras and Iliadis, 2006). Such a phenomenon is taken into account by Kervinen and Yliruusi (1993), where the authors assume a lag time during which possible coating of the tablet or some surface potential prevents the beginning of wetting and also dissolution thus the probability of any molecule to become dissolved is zero. After the lag time, changes on the surface of the tablet appear until the transition layer is formed. In this stage, probability of the particles to enter the solute grows until the system is in such a state that all remaining drug molecules have the same probability to become dissolved and the dissolution follows the first order kinetics.

In this study we employ a different approach, compared to Kervinen and Yliruusi (1993), for describing the same phenomenon. It is based on consideration of a random lag time after which the diffusion layer is formed and the process of dissolution itself begins. In contrast to above mentioned paper (Kervinen and Yliruusi, 1993), we assume that the homogeneous phase appears directly after the lag time without any progressive phase. Even this simplified assumption of initial transient phase has significant impact on the model behavior. The obtained dissolution profiles have sigmoidal shape similarly to those presented by Kervinen and Yliruusi (1993) and in addition, taking into account measurement errors, the model can explain typical shapes of variability observed in dissolution data (see Elkoshi, 1997). Finally, the approach offers a simple physical explanation or at least approximation for commonly used Weibull model.

2. Methods

Standard description of dissolution process is by fraction of drug dissolved up to time t , $F(t) = A(t)/D$, where $A(t)$ denotes the amount of drug dissolved up to time t and D is the initial dose. Function $F(t)$, called dissolution profile, is monotonously increasing from zero to an asymptote lower or equal to one and thus, after a proper scaling if the asymptote is lower than one, it can be seen as a cumulative distribution function of a random variable T representing the time until a randomly selected molecule enters solution. Example

* Corresponding author at: Department of Mathematics and Statistics, Faculty of Science, Masaryk University, Kotlarska 2, 611 37 Brno, Czech Republic. Tel.: +420 549 49 5331.

E-mail addresses: cupera@ics.muni.cz, xcupera@mail.muni.cz (J. Cupera), lansky@biomed.cas.cz (P. Lansky).

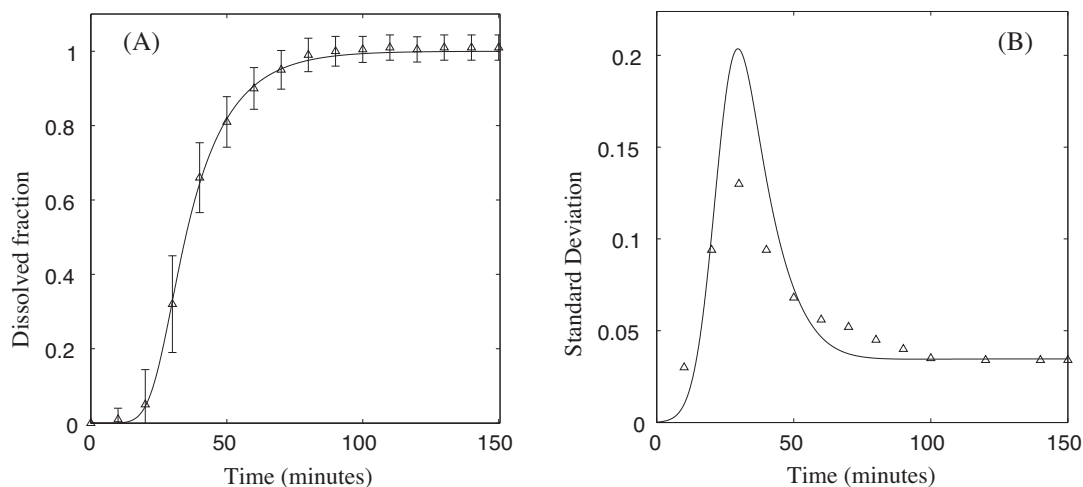


Fig. 1. Experimental dissolution data taken from Elkoshi (1997). (A) Dissolution profile given by Gaussian lag time model (16), $1/\lambda = 14.93$ [min], $t_0 = 23.61$ [min], $\sigma_{t_0} = 5.35$ [min] (best fit), with mean experimental data (triangle) and indicated standard deviation, $CV(T) = 0.41$. (B) Experimental standard deviation (triangle) and standard deviation $s(t)$ given in (15). The parameters λ , t_0 and σ_{t_0} are the same as in (A) and parameter $\sigma_D = 0.035$, standard deviation tends to σ_D for large t .

of dissolution profile can be seen Fig. 1A. Statistical moments of the random variable T can be derived from $F(t)$,

$$ET^n = n \int_0^\infty t^{n-1} (1 - F(t)) dt, \tag{1}$$

see Weiss (1991), namely we obtain mean dissolution time, $MDT = ET$ and variance, $VarT = ET^2 - (ET)^2$. The dimensionless standard deviation,

$$CV(T) = \frac{\sqrt{VarT}}{MDT}, \tag{2}$$

is also called coefficient of variation (CV).

Many dissolution profiles have been proposed to describe the dissolution patterns, for reviews see Costa and Lobo (2001), Dokoumetzidis and Macheras (2006), Lansky and Weiss (2003), and Macheras and Iliadis (2006). To compare the models with the data, two measures are commonly employed (see Moore and Flanner, 1996): the difference factor f_1 and the similarity factor f_2 . The difference factor, f_1 , measures the percent error between the two curves and is proportional to the average difference between the two profiles,

$$f_1 = 100 \frac{\sum_{i=1}^N |R(t_i) - T(t_i)|}{\sum_{i=1}^N R(t_i)}, \tag{3}$$

where N is number of samples, $R(t_i)$ and $T(t_i)$ are the dissolved percent of the reference and test product respectively at the time t_i . The percent error is zero when both test and reference product coincide and increase proportionally with the dissimilarity between the two dissolution profiles.

The similarity factor, f_2 , is inversely proportional to the average squared difference between the two profiles, with emphasis on the larger difference among all the time-points and measuring the closeness between the two profiles,

$$f_2 = 50 \log \left(\frac{100}{\sqrt{1 + (1/N) \sum_{i=1}^N (R(t_i) - T(t_i))^2}} \right), \tag{4}$$

where $R(t_i)$ and $T(t_i)$ are defined as above, N is number of samples. The similarity factor takes values between 0 and 100, where the value 100 is reached when the dissolution profiles coincide and tends to zero as the dissimilarity increases.

2.1. Homogeneous model of dissolution

The basic model of dissolution, presented by Noyes and Whitney (1897), and called homogeneous or the first-order model, is described by exponential distribution function of the random variable T ,

$$F_H(t) = 1 - \exp(-\lambda t), \quad t \geq 0, \tag{5}$$

where $\lambda > 0$ is a rate constant and index H stands for *homogeneous*. For the mean dissolution time and variance holds

$$MDT = \frac{1}{\lambda}, \quad VarT = \frac{1}{\lambda^2}. \tag{6}$$

For sake of clarity, Eq. (6) is valid if the amount of drug needed to saturate the dissolution medium is equal (preferably higher) to the dose utilized. In all other cases, MDT depends on the solubility dose ratio (see Rinaki et al., 2003). Model (5) is characterized by the CV equal to one. Note that Eq. (5) was derived from an experiment which configuration ensured the homogeneous conditions, see Noyes and Whitney (1897). The authors also attributed the mechanism of dissolution to a thin transition (diffusion) layer which is formed around the solid surface and through which the molecules diffuse into the solute.

2.2. Random lag time model of dissolution

The homogeneous model of dissolution has the initial time instant always set to zero. In order to bring the model closer to reality we take into account a random delay until the diffusion layer is created. Let us assume that the time T when a randomly selected molecule enters solution is given by equation

$$T = T_0 + T_H, \tag{7}$$

where T_0 describes lag time until the transition layer on the surface of the tablet is created and T_H is the dissolution time starting from the moment when the conditions for the homogeneous dissolution are established. Random variables T_0 and T_H are assumed to be independent and thus we can easily derive statistical properties of T ,

$$MDT = ET_0 + \frac{1}{\lambda}, \quad VarT = VarT_0 + \frac{1}{\lambda^2}, \tag{8}$$

and by substituting (8) into definition (2) we obtain

$$CV(T) = \frac{\sqrt{1 + \lambda^2 \text{Var}T_0}}{1 + \lambda \text{E}T_0} \tag{9}$$

One can see, that assuming the existence of the random lag time changes stochastic properties of homogeneous model (5). Formally, the CV can take an arbitrary value in dependency on the statistical properties of random variable T_0 . However, inequality $CV(T) > 1$ is satisfied if and only if

$$CV(T_0) > \sqrt{1 + \frac{2}{\lambda \text{E}T_0}} \tag{10}$$

If we assume that the dissolution itself is much shorter than time needed for creating the conditions for it, i.e. $1/\lambda = \text{E}T_H \ll \text{E}T_0$, then $CV(T) > 1$ is equivalent to $CV(T_0) > 1$. On the other hand, it can be easily verified that inequality $CV(T_0) < 1$ implies inequality $CV(T) < 1$ independently of other statistical properties of T_0 .

Eqs. (8) and (9) describe only the moments of the dissolution time. To obtain the complete dissolution profile we have to consider the dissolution profile of the homogeneous part and probabilistic properties of the random lag time. Let us assume, that the lag time T_0 is characterized by its cumulative distribution function $\Psi(t) = \text{Prob}(T_0 \leq t)$ defined for $t \geq 0$. Then, probability density of T can be calculated as a convolution of exponential density (as follows from (5)) and $\psi(t)$ which is the density corresponding to $\Psi(t)$,

$$f(t) = \int_0^t \lambda \exp(-\lambda(t-u))\psi(u)du, \tag{11}$$

from which the dissolution profile follows,

$$F(t) = \Psi(t) - \int_0^t \exp(-\lambda(t-u))\psi(u)du, \tag{12}$$

as can be verified by taking the derivative of (12) with respect to t . Function $F(t)$ is the cumulative distribution function of random variable (7) thus it is monotonically increasing and approaching asymptote equal to one. Furthermore, it can be seen from (11) that $F(0) = f(0) = 0$ and thus the dissolution profile (12) has always the sigmoidal shape. This will be illustrated on several examples (see Figs. 3A, 4A and 5A). It will be also shown that for certain distributions of T_0 function (12) an approximate Weibull function and thus to serve as a simple reasoning behind its application.

2.3. Statistical properties of repeated measurements

Model introduced in the previous subsection permits to find statistical properties of repeatedly measured dissolution data. A typical feature of any deterministic model is that for identical initial conditions and the same values of parameters, its sample paths coincide. On the contrary, the experimental data show variability at each time instant of the observation whatever effort is made to keep the conditions stable. This variability was theoretically studied by Elkoshi (1997), where the author investigated functions describing the variability in time which originated from Weibull model (see Section 3.4). In our recent paper Cupera and Lansky (2010), we divided the sources of variability into two types – the variability due the measurement errors and the temporal variability in the dissolution vessel environment. The complete variability of the dissolution data is then taken as a sum of these two components. In the next we show that there may exist another source of variability obtained by assuming random initial transient phase in the drug dissolution. Furthermore, it may explain the ‘nose’ shape of standard deviation of the measured dissolved fraction that can be observed in experimental data, see Fig. 1B.

Random variable T given by (7) follows the first order kinetics described by random variable T_H after the lag time T_0 elapses.

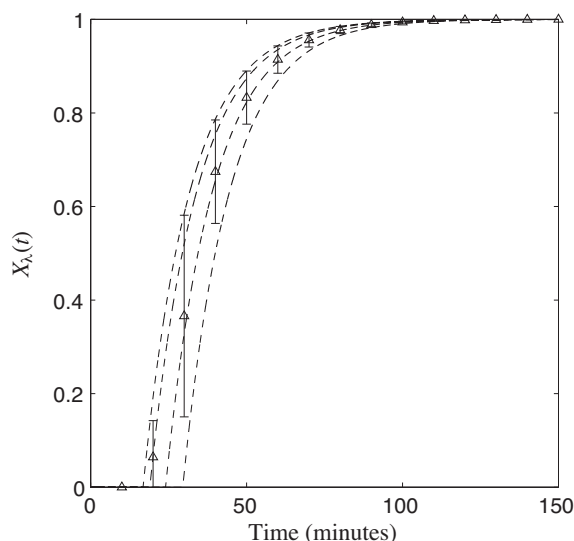


Fig. 2. Four realizations of random variable $X_\lambda(t)$ given by (13) in dependency on time t and $\lambda = 1/25$ (dashed). Sample means (triangle) and standard deviations are indicated.

Hence for given realization of T_0 , the random variable T is described by homogeneous dissolution profile (5) with origin shifted to a realization of T_0 . Thus model (7) can be equivalently described by the amount of dissolved fraction at the time instant t ,

$$X_\lambda(t) = 1 - \exp(-\lambda(t - T_0)), \quad t \geq T_0, \tag{13}$$

which is a family of random variables depending on time t and parameter λ , see Fig. 2, and

$$\Theta(x; t, \lambda) = \text{Prob}(X_\lambda(t) \leq x) = \text{Prob}\left(T_0 > \frac{\ln(1-x)}{\lambda} + t\right) = 1 - \Psi\left(\frac{1}{\lambda} \ln(1-x) + t\right) \tag{14}$$

defined for $x \in [0, 1]$ is corresponding cumulative distribution function. This function is monotonically increasing from $\Theta(0; t, \lambda) = 1 - \Psi(t)$ to $\Theta(1; t, \lambda) = 1$. It allows us to calculate statistical moments of random variables $X_\lambda(t)$, namely mean $\text{E}X_\lambda(t)$ and variability $\text{Var}X_\lambda(t)$, for details see Appendix A. As expected, we obtain $\text{E}X_\lambda(t) = F(t)$, where $F(t)$ is dissolution profile (12) derived in previous subsection for model (7).

The possibility to obtain variability directly from model and without any additional parameters is unique among other models of dissolution. However, as mentioned, another source of variability affecting the experimental data is due to measuring instruments always showing errors that are commonly supposed to be proportional to the actual values. As shown in Cupera and Lansky (2010), the function describing variability in data caused by measurement errors is proportional to the square of the dissolution profile. There is no reason to expect that the measurement error depends on the random lag time, thus we obtain a complete function $s^2(t)$ describing variability of dissolved fraction as a sum of the two variabilities,

$$s^2(t) = \text{Var}X_\lambda(t) + \sigma_D^2 F^2(t), \tag{15}$$

where σ_D determines level of measurement errors and $F(t)$ is given by (12). It can be seen in Figs. 3B, 4B and 5B have the ‘nose’ shape as shown in Fig. 1B and thus the derived function can explain the typical shape of variability observed in dissolution data (see e.g. Elkoshi, 1997).

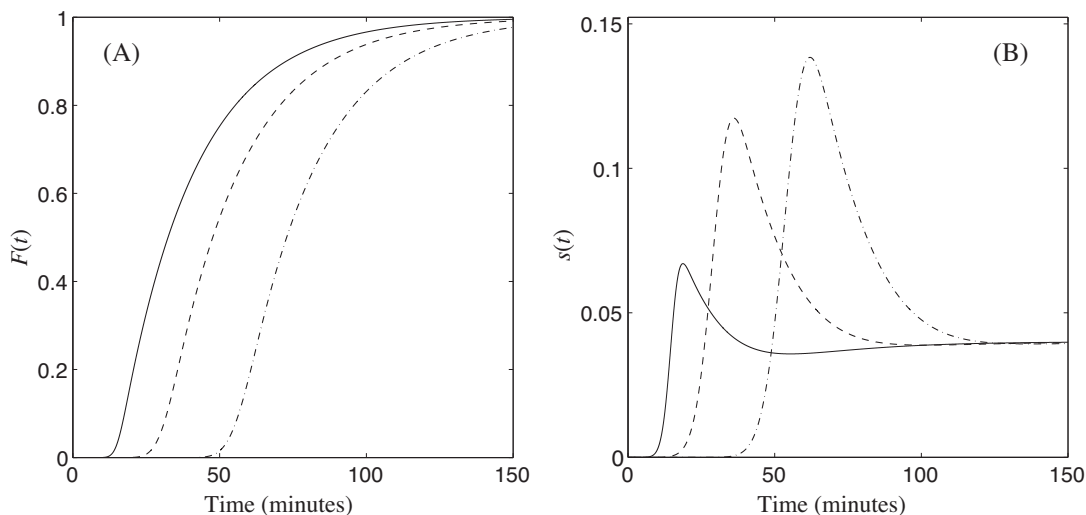


Fig. 3. Properties of dissolution model with Gaussian distribution of the lag time. (A) Dissolution profile $F(t)$ given by (16), the parameters are $t_0 = 15$, $\sigma_{t_0} = 2$ (solid), resp. $t_0 = 30$, $\sigma_{t_0} = 4$ (dashed), resp. $t_0 = 55$, $\sigma_{t_0} = 5$ (dash-dotted). Rate constant of dissolution in homogeneous phase is $\lambda = 1/25$, (B) corresponding standard deviation of measured data (15) with measurement errors taken into account, parameter $\sigma_D = 0.04$ and the rest of the parameters is taken as in (A).

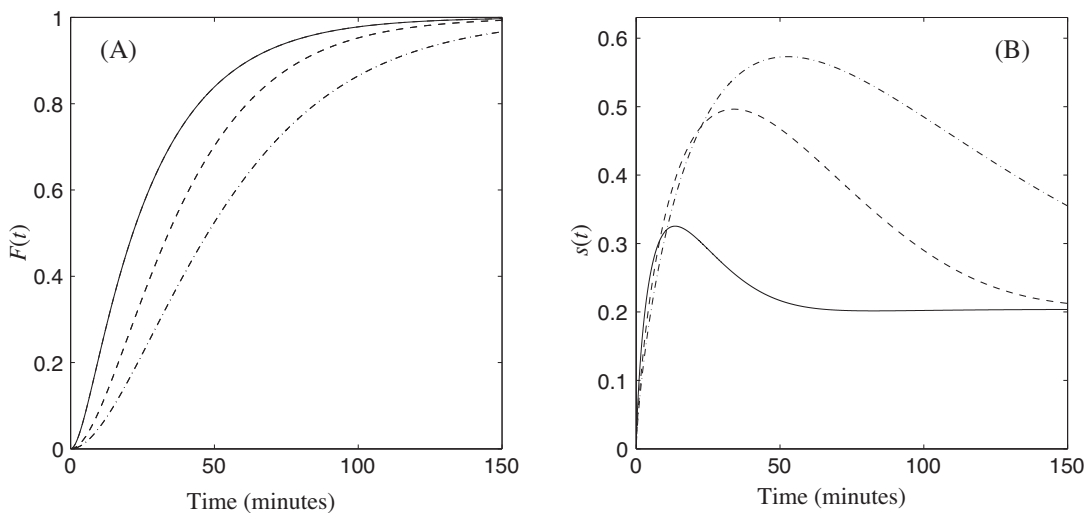


Fig. 4. Properties of dissolution model with exponential distribution of the lag time. (A) Dissolution profile $F(t)$ given by (18), the parameters are $t_0 = 4$ (solid), resp. $t_0 = 16$ (dashed), resp. $t_0 = 32$ (dash-dotted). Rate constant of dissolution in homogeneous phase is $\lambda = 1/25$, (B) corresponding standard deviation of measured data (15) with measurement errors taken into account, parameter $\sigma_D = 0.04$ and the rest of the parameters is taken as in (A).

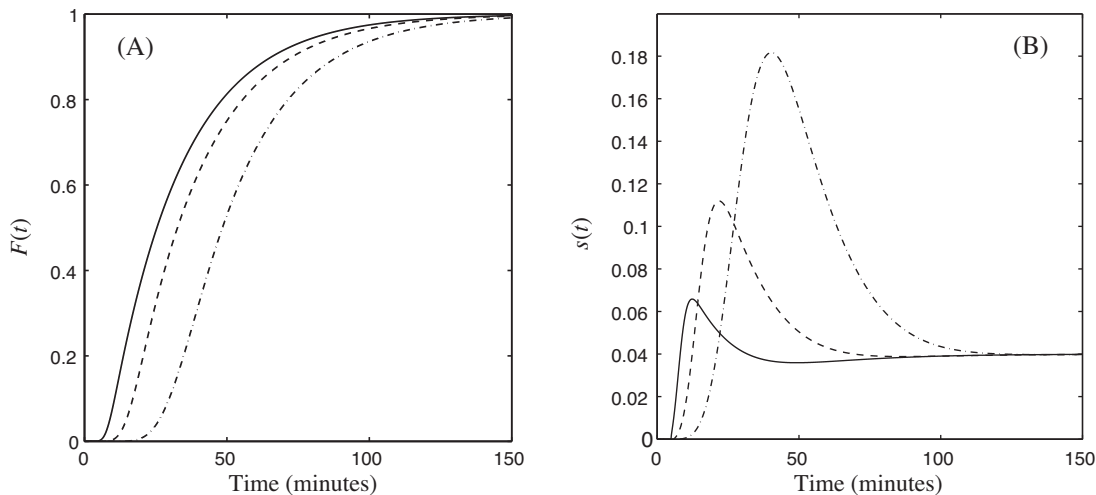


Fig. 5. Properties of dissolution model with Gamma distribution of the lag time. (A) Numerically calculated dissolution profiles $F(t)$, the parameters of (19) are $t_0 = 8$, $a = 2$ (solid), resp. $t_0 = 15$, $a = 1$ (dashed), resp. $t_0 = 30$, $a = 0.5$ (dash-dotted). Rate constant of dissolution in homogeneous phase is $\lambda = 1/25$, (B) corresponding standard deviation of measured data (15) with measurement errors taken into account, parameter $\sigma_D = 0.04$ and the rest of the parameters is taken as in (A).

3. Results

Three types of random lag time are proposed and investigated in this section. Finally, the model is related to Weibull dissolution function.

3.1. Gaussian lag time

Based on the law of large numbers we can expect that the initial time T_0 is normally distributed with mean t_0 and variance $\sigma_{t_0}^2$, $T_0 \sim N(t_0, \sigma_{t_0}^2)$. Due to the properties of Gaussian distribution we have to assume that $t_0 > 0$ and $\sigma_{t_0} \ll t_0$ in order to eliminate negative realizations of random variable T_0 . Dissolution profile (12) can be calculated,

$$F(t) = \Phi\left(\frac{t-t_0}{\sigma_{t_0}}\right) - \Phi\left(\frac{t-t_0}{\sigma_{t_0}} - \lambda\sigma_{t_0}\right) \exp\left(-\lambda(t-t_0) + \frac{\lambda^2\sigma_{t_0}^2}{2}\right), \quad (16)$$

where $\Phi(\cdot)$ is cumulative distribution function of standard normal (Gaussian) distribution, for an example see Fig. 3A. In the figure can be also seen standard deviation $s(t)$ (square root of variability) given by (15).

The CV of model (16) can be formally greater than one for some combination of parameters t_0 and σ_{t_0} . However, inserting $ET_0 = t_0$ and $\text{Var}T_0 = \sigma_{t_0}^2$ into (9) and imposing $\text{CV}(T) < 1$ gives

$$\sigma_{t_0} < \sqrt{t_0^2 + \frac{2t_0}{\lambda}}. \quad (17)$$

Our assumptions imply $\sigma_{t_0} \ll t < (t_0^2 + 2t_0/\lambda)^{1/2}$ and thus the CV is always lower than one for model of dissolution given by (16).

The Gaussian lag time model was used to fit the data in Fig. 1. Function (16) fits the dissolution data well, the difference factor $f_1 = 1.25$ and similarity factor $f_2 = 92.49$. The standard deviation also successfully describes the data, however, the model predicts higher standard deviation at the maximum than observed which may be caused by inappropriate choice of probability distribution of the lag time or by assumption of homogeneous conditions during the experiment.

3.2. Exponential lag time

Assuming that the changes on the surface follow the homogeneous model implies T_0 following model (5) with $\lambda = 1/t_0$ in order to ensure $ET_0 = t_0$. Dissolution profile (12) has form

$$F(t) = 1 - \frac{t_0}{1 - \lambda t_0} \left(\frac{1}{t_0} \exp(-\lambda t) - \lambda \exp\left(-\frac{t}{t_0}\right) \right) \quad (18)$$

for $t \geq 0$. This model was already derived using entirely different approach as a special case of heterogeneous model of dissolution (see Lansky and Weiss, 2001). It is also known as a bi-exponential model utilized, for example, in Alway et al. (1996) and Allahham and Stewart (2007). Model (18) is not suitable to fit the dissolution data shown in Fig. 1, the difference is $f_1 = 8.59$ and similarity $f_2 = 53.77$. However, the model was successfully used to fit experimental dissolved fractions in above mentioned papers. The function (18) is depicted in Fig. 4A. In the figure can be also seen standard deviation $s(t)$ (square root of variability) given by (15). It can be easily verified that the CV of model (18) is always lower than one.

3.3. Gamma lag time

The previous two examples were based on simple assumptions for the lag time. Their main advantage was that they resulted

in the analytical expressions for the quantities of interest. More realistic situation is obtained by assuming gamma distribution of T_0 ,

$$\psi(t) = \frac{a^{at_0}}{\Gamma(at_0)} t^{at_0-1} \exp(-at), \quad t \geq 0, \quad (19)$$

where $ET_0 = t_0$, $a > 0$ is constant and $\Gamma(\cdot)$ denotes the gamma function. For special values of parameters a and t_0 both previous cases are practically included. Unfortunately, the dissolution profile (12) and variability (24) can be obtained only numerically in the model. In Fig. 5A are shown different shapes of dissolution profile (12) together with corresponding standard deviations $s(t)$ related to variance (15) shown in Fig. 5B. It can be seen that, similarly to the previous examples, the dissolution profile shows the sigmoidal shape and the standard deviation has the 'nose'. The CV is greater than one if and only if $at_0 < 1$ and

$$\lambda \left(\frac{1}{a} - t_0 \right) > 2. \quad (20)$$

Model of dissolution with gamma lag time can be used to fit the data shown in Fig. 1 equally well as the Gaussian lag time model does; the difference factor is $f_1 = 1.33$ and the similarity factor is $f_2 = 91.97$. The estimated curves are not visually distinguishable from those obtained for the Gaussian model shown in Fig. 1.

3.4. Approximation of the Weibull model

The standard descriptors of dissolution data are, for example, the cubic root law, the square root time equation and some modifications of the simple exponential function (see e.g. Costa and Lobo, 2001; Dokoumetzidis and Macheras, 2006; Macheras and Iliadis, 2006), however, these models do not describe sigmoidal shape of dissolution patterns. Simultaneously, one of the most successful model in fitting experimental data having sigmoidal shape is, similarly to our model, the Weibull model,

$$F_W(t) = 1 - \exp(-rt^h), \quad t \geq 0, \quad (21)$$

where $r > 0$, $h > 0$ are constants. Parameter r determines scale of the profile whereas parameter h influences the shape. As the Weibull model is only descriptive and has not been deduced from any fundamental physical law, it has been the subject of some criticism. (Costa and Lobo, 2001), summarized these arguments such as lack of any kinetic background, or that the model has not any single parameter related to the intrinsic dissolution rate of the solvent. Papadopoulou et al. (2006) provided experimental evidence for the successful use of the Weibull function in drug release studies. Result of their study links values of parameter h and the diffusion mechanism of the release. Authors succeeded in the case $h \leq 1$, but for parameter h having value greater than one, which implies the sigmoidal shape of function (21), the dissolution is generally assigned to 'complex release mechanism'. In the next we show that for all values $h \geq 1$ the Weibull function (21) can be sufficiently well approximated by the model with the initial transient phase. For $h < 1$ the Weibull model has not sigmoidal shape and is not suitable for approximation by lag time model.

To quantify the approximation we use the integrated square error (ISE),

$$\text{ISE}(F, F_W) = \int_0^\infty (F_W(t) - F(t))^2 dt, \quad (22)$$

where $F_W(t)$ is Weibull model (21) and $F(t)$ is dissolution profile of the model with initial transient phase. For the Weibull model with parameters r and h fixed we minimize function (22) with respect to the parameters of Gaussian (16) and gamma lag time model in order to obtain the best approximation of the Weibull function (21). As the integral (22) can not be obtained analytically, we employ

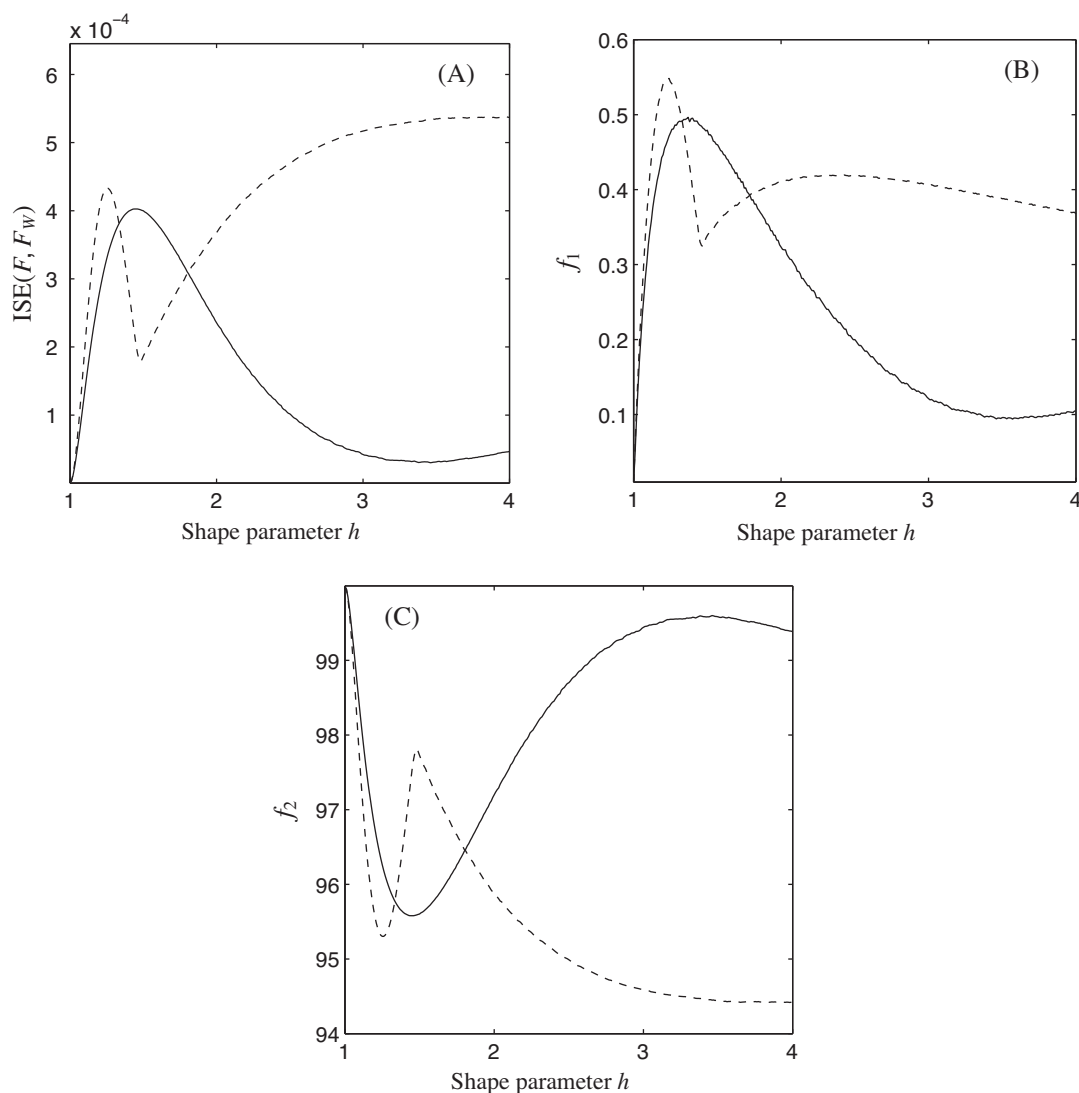


Fig. 6. Integrated square error, similarity and difference between Weibull function (21) and Gaussian lag time model (16) (solid) and gamma lag time model (dashed). The scale parameter r of Weibull function is fixed, $r = 1$, shape parameter h is variable, $1 \leq h \leq 4$, $\Delta h = 0.01$. Parameters determining lag time models are obtained by minimizing (22) for given r and h . (A) Dependence of minimal ISE (22) on the value of parameter h . (B) The difference factor f_1 given by (3), where $R(t_i) = 100F_W(t_i)$ and $T(t_i) = 100F(t_i)$, $F_W(t_i)$ is Weibull model (21), $F(t_i)$ is given lag time model with minimal ISE and t_i are equidistant times taken from 0 to the time when 99% is dissolved, $\Delta t_i = 0.01$. (C) Value of the similarity factor f_2 given by (4) where $R(t)$ and $T(t)$ are taken as in (B).

numeric approach with time step $\Delta t = 0.01$ and t between 0 and the time when more than 99% of the drug is dissolved in both Weibull and lag time model. The minimal ISE's (22) for the lag time models and Weibull model with parameter r fixed, $r = 1$, and different values of parameter $h \in [1, 4]$ with step $\Delta h = 0.01$ are shown in

Fig. 6A. It can be seen that for $1 \leq h \leq 1.33$ the results are relatively similar, however, the Gaussian model (16) has slightly lower ISE than the gamma one. For h between 1.33 and 1.8 the lowest error has the gamma lag time model and for $h > 1.8$ the best results are again obtained for the Gaussian lag time model (16). The ISE is always lower than 6×10^{-4} for both models. The exponential lag time model (18) is not shown here because its dissolution profile with minimal ISE coincide with gamma lag time model for $h < 1.48$ and thus the ISE is also the same. It means that the exponential model is more suitable in this case as it has simple analytical form in contrast to gamma lag time model. On the contrary, for h greater than 1.48 the minimal ISE of model (18) rapidly increase with increasing h and thus the exponential lag time model (18) is

not suitable for approximation by Weibull model with such shape parameter.

To show similarity, resp. difference between dissolution profiles of Gaussian and gamma lag time models having minimal ISE and corresponding Weibull function we employ the approaches summarized in Section 2. We take equidistant time points t_i with time step $\Delta t = 0.01$ from zero to the time when more than 99% is dissolved in both Weibull and lag time models. We insert $R(t_i) = 100F_W(t_i)$ as the reference product and $T(t_i) = 100F(t_i)$ as the test product into Eqs. (3) and (4). The function $F(t_i)$ is given by Gaussian lag time model (16) and numerically calculated gamma lag time model presented in Section 3.3, both having minimal ISE (22) with respect to Weibull model (21) with fixed parameters. The results for $r = 1$ and different values of parameter $h \in [1, 4]$ with step $\Delta h = 0.01$, are shown in Fig. 6B and C. It can be seen, that the shapes of f_1 and f_2 in dependency on h follows the shape of ISE, thus the highest similarity, resp. lowest difference is obtained for the models with lowest ISE as discussed above. The similarity is always greater

than 94%, resp. difference is lower than 0.5% thus the lag time models of dissolution can approximate the Weibull function well.

4. Discussion

We presented a new model of dissolution based on the homogeneous one but in addition extended for the initial transient phase. This extension is realistic and can explain the sigmoidal shape of dissolution patterns. Furthermore, for Gaussian and gamma distribution of the lag time the proposed model can successfully approximate the Weibull function and thus to serve as a reasoning behind its widespread application. Our approach also divides the resulting statistical properties (MDT, variability) of the dissolution time into the properties of the lag time and that of the dissolution time itself. It means, for example, the MDT of the dissolution process is different from that commonly calculated directly from the data where the lag time is not taken into account.

The main advantage of the proposed model is that it offers a function of variability, resp. standard deviation of the repeated measurements, which has the commonly observed shape. Furthermore, for the complete estimation of the standard deviation only the parameters obtained by fitting the dissolution profile to the data are needed. This is in contrast to other proposed functions (Cupera and Lansky, 2010; Elkoshi, 1997) which depend on additional parameters. Only free parameter of the proposed function is describing the level of measurement errors and it can be easily estimated from data measured at the moment when entire amount of the drug is dissolved or the solute becomes saturated.

In the data on which we illustrate the proposed model, it predicts higher standard deviation at the maximum than is its actual value (Fig. 1B). If this feature is a typical drawback of the model or just a singular case cannot be deduced from the single example. It also may be caused by inappropriate choice of probability distribution of the lag time, resp., by assumption of homogeneous conditions during the dissolution itself. More serious disadvantage of the model is that its analytical form (the dissolution profile and the variability of the repeated measurements) is of rather complicated form and the fit to the experimental data can be tedious. The analytical solution may even be unavailable for a number of probability distributions of the lag time, similarly to the gamma lag time model presented in Section 3.3. The only way how to overcome the problem is implementation of the model into an appropriate computer software and application of sophisticated numerical methods.

In our model (8) the homogeneous phase appears directly after the lag time, but also during the creation of transitional layer on the surface, the drug particles diffuse from the tablet to the bulk aqueous phase. Including this into the model would make it more realistic, on one side, but less tractable on the other. We have to keep in mind that any applicable model should be a compromise between going to the reality as close as possible and tractability. Similarly, the assumption of the homogeneous conditions may not be relevant and taking, for example, Hixson-Crowell (see Macheras and Iliadis, 2006) or a reaction limited model of dissolution (see e.g. Dokoumetzidis et al., 2008; Lansky and Weiss, 1999) instead of the homogeneous one can evoke entirely new class of dissolution models incorporating the initial transient phase.

Acknowledgements

This work was supported by Center for Theoretical and Applied Statistics LC06024 and Research project AV0Z50110509.

Appendix A.

Probability density corresponding to cumulative distribution function (14) of repeated measurements has form

$$\theta(x; t, \lambda) = \frac{\psi\left(\frac{1}{\lambda} \ln(1-x) + t\right)}{\lambda(1-x)} + \delta(x)(1 - \Psi(t)), \quad (23)$$

for $x \in [0, 1]$, where $\delta(x)$ is a Dirac delta function. The first term in formula (23) describes probability density of dissolved fractions related to profiles that started up to the time t only and thus its integral may not to be equal to one. The second term, $\delta(x)(1 - \Psi(t))$, covers the dissolution profiles that start after the time t and thus their value is zero at given time instant. Mean of random variable (13) can be calculated from (23). As it holds $\int_{-\infty}^{\infty} x\delta(x)dx = 0$ we obtain

$$\begin{aligned} EX_{\lambda}(t) &= \int_0^1 \frac{x}{\lambda(1-x)} \psi\left(\frac{1}{\lambda} \ln(1-x) + t\right) dx \\ &= \int_{-\infty}^t (1 - \exp(\lambda(u-t))) \psi(u) du \\ &= \Psi(t) - \int_{-\infty}^t \exp(-\lambda(t-u)) \psi(u) du, \end{aligned}$$

where substitution $u = \ln(1-x)/\lambda + t$ is applied in the second step and $\Psi(t) = \int_{-\infty}^t \psi(u) du$ is cumulative distribution function corresponding to density $\psi(t)$. Similarly we can calculate the second moment, $EX_{\lambda}(t)^2$, and variability of the dissolved fraction at the time t in form

$$\begin{aligned} \text{Var}X_{\lambda,t} &= \Psi(t)(1 - \Psi(t)) - 2 \exp(-\lambda t)(1 - \Psi(t))L(1, t) \\ &\quad + \exp(-2\lambda t)(L(2, t) - L^2(1, t)), \end{aligned} \quad (24)$$

where

$$L(q, t) = \int_0^t \exp(q\lambda u) \psi(u) du. \quad (25)$$

For example, if random variable T_0 has Gaussian distribution with mean t_0 and variability $\sigma_{t_0}^2$, then

$$L(q, t) = \exp\left(\frac{1}{2}\lambda^2 q^2 \sigma_{t_0}^2 + \lambda q t_0\right) \Phi\left(\frac{t-t_0}{\sigma_{t_0}} - q\lambda\sigma_{t_0}\right), \quad (26)$$

and if T_0 is exponentially distributed with mean t_0 , then

$$L(q, t) = \frac{1 - \exp(q\lambda t - t/t_0)}{1 - q\lambda t_0}. \quad (27)$$

For T_0 following Gamma distribution the function $L(q, t)$ can not be obtained analytically.

References

- Allahham, A., Stewart, P.J., 2007. Enhancement of the dissolution of indomethacin in interactive mixtures using added fine lactose. *Eur. J. Pharm. Biopharm.* 67, 732–742.
- Alway, B., Sangchantra, R., Stewart, P.J., 1996. Modelling the dissolution of diazepam in lactose interactive mixtures. *Int. J. Pharm.* 130, 213–224.
- Costa, P., Lobo, J.M.S., 2001. Modeling and comparison of dissolution profiles. *Eur. J. Pharm. Sci.* 13, 123–133.
- Cupera, J., Lansky, P., 2010. Random effects in drug dissolution. *Eur. J. Pharm. Sci.* 41, 430–439.
- Dokoumetzidis, A., Macheras, P., 2006. A century of dissolution research: from Noyes and Whitney to the biopharmaceutics classification system. *Int. J. Pharm.* 321, 1–11.
- Dokoumetzidis, A., Papadopoulou, V., Valsami, G., Macheras, P., 2008. Development of a reaction-limited model of dissolution: Application to official dissolution tests experiments. *Int. J. Pharm.* 255, 114–125.
- Elkoshi, Z., 1997. On the variability of dissolution data. *Pharm. Res.* 10, 1355–1362.
- Kervinen, L., Yliruusi, J., 1993. Modelling s-shaped dissolution curves. *Int. J. Pharm.* 92, 115–122.

- Lansky, P., Weiss, M., 1999. Does the dose solubility ratio affect the mean dissolution time of drugs? *Pharm. Res.* 16, 1470–1478.
- Lansky, P., Weiss, M., 2001. Modeling heterogeneity of particles and random effects in drug dissolution. *Pharm. Res.* 18, 1061–1067.
- Lansky, P., Weiss, M., 2003. Classification of dissolution profiles in terms of fractional dissolution rate and a novel measure of heterogeneity. *J. Pharm. Sci.* 8, 1632–1647.
- Macheras, P., Iliadis, A., 2006. *Modeling in Biopharmaceutics, Pharmacokinetics and Pharmacodynamics*. Springer-Verlag, Berlin.
- Moore, J.W., Flanner, H., 1996. Mathematical comparison of dissolution profiles. *Pharm. Technol.* 20, 64–74.
- Noyes, A.A., Whitney, W.R., 1897. Über die auflösungsgeschwindigkeit von festen stoffen in ihren eigenen lösungen. *Z. Phys. Chem.* 13, 689–692.
- Papadopoulou, V., Kosmidis, K., Vlachou, M., Macheras, P., 2006. On the use of the weibull function for the discernment of drug release mechanisms. *Int. J. Pharm.* 309, 44–50.
- Polli, J.E., Rekhi, G.S., Augsburger, L.L., Shah, V.P., 1997. Methods to compare dissolution profiles and a rationale for wide dissolution specification for metoprolol tablets. *J. Pharm. Sci.* 6, 690–700.
- Rinaki, E., Dokoumetzidis, A., Macheras, P., 2003. The mean dissolution time depends on the dose/solubility ratio. *Pharm. Res.* 20, 406–408.
- Weiss, M., 1991. Residence time distributions in pharmacokinetics: behavioral and structural models. In: *Advanced Methods of Pharmacokinetics and Pharmacodynamic System Analysis*. Plenum Press, New York, pp. 89–101.